

1 **Particle acidity and sulfate production during severe haze events in China**
2 **cannot be reliably inferred by assuming a mixture of inorganic salts**

3
4 Gehui Wang^{1,2,3,*}, Fang Zhang^{4,5}, Jianfei Peng^{5,6}, Lian Duan^{5,7}, Yuemeng Ji^{5,8}, Wilmarie
5 Marrero-Ortiz⁵, Jiayuan Wang², Jianjun Li², Can Wu², Cong Cao², Yuan Wang⁹, Jun Zheng¹⁰,
6 Jeremiah Secrest⁵, Yixin Li⁵, Yuying Wang^{4,5}, Hong Li¹¹, Na Li^{5,12}, and Renyi Zhang^{5,6*}

7
8 ¹Key Laboratory of Geographic Information Science of the Ministry of Education, School of
9 Geographic Sciences, East China Normal University, Shanghai 200241, China

10 ²State Key Laboratory of Loess and Quaternary Geology, Institute of Earth Environment, China
11 Academy of Sciences, Xi'an 710061, China

12 ³Center for Excellence in Regional Atmospheric Environment, Institute of Urban Environment,
13 Chinese Academy of Science, Xiamen, China

14 ⁴Beijing Normal University, Beijing 100875, China

15 ⁵Departments of Atmospheric Sciences and Chemistry, Texas A&M University, College Station,
16 TX, 77843, USA

17 ⁶State Key Joint Laboratory of Environmental Simulation and Pollution Control, College of
18 Environmental Sciences and Engineering, Peking University, Beijing 100871, China

19 ⁷East China University of Science and Technology, Shanghai, China

20 ⁸School of Environmental Science and Engineering, Institute of Environmental Health and
21 Pollution, Control, Guangdong University of Technology, Guangzhou 510006, China

22 ⁹Jet Propulsion Laboratory, California Institute of Technology, Pasadena, CA 91125, USA

23 ¹⁰Jiangsu Key Laboratory of Atmospheric Environment Monitoring and Pollution Control,
24 Nanjing University of Information Science & Technology, Nanjing 210044, China

25 ¹¹State Key Laboratory of Environmental Criteria and Risk Assessment, Chinese Research
26 Academy of Environmental Sciences, Beijing 100012, China

27 ¹²Key Laboratory of Songliao Aquatic Environment, Jilin Jianzhu University, Changchun,
28 130118, China

29
30
31
32
33 *Corresponding author:

34 Prof. Gehui Wang, E-mail : ghwang@geo.ecnu.edu.cn, or wanggh@ieecas.cn

35 Prof. Renyi Zhang, E-mail: renyi-zhang@tamu.edu

37 **Abstract:** Atmospheric measurements showed rapid sulfate formation during severe haze
38 episodes in China, with fine particulate matter (PM) consisting of a multi-component mixture
39 that is dominated by organic species. Several recent studies using the thermodynamic model
40 estimated the particle acidity and sulfate production rate, by treating the PM exclusively as a
41 mixture of inorganic salts dominated by ammonium sulfate and neglecting the effects of organic
42 compounds. Noticeably, the estimated pH and sulfate formation rate during pollution periods in
43 China were highly conflicting among the previous studies. Here we show that a particle mixture
44 of inorganic salts adopted by the previous studies does not represent a suitable model system and
45 that the acidity and sulfate formation cannot be reliably inferred without accounting for the
46 effects of multi-aerosol compositions during severe haze events in China. Our laboratory
47 experiments show that SO₂ oxidation by NO₂ with NH₃ neutralization on fine aerosols is
48 dependent on the particle hygroscopicity, phase-state, and acidity. Ammonium sulfate and oxalic
49 acid seed particles exposed to vapors of SO₂, NO₂, and NH₃ at high relative humidity (RH)
50 exhibit distinct size growth and sulfate formation. Aqueous ammonium sulfate particles exhibit
51 little sulfate production, in contrast to aqueous oxalic acid particles with significant sulfate
52 production. Our field measurements demonstrate significant contribution of water-soluble
53 organic matter to fine PM in China and indicate that the use of oxalic acid in laboratory
54 experiments is representative of ambient organic dominant aerosols. While the particle acidity
55 cannot be accurately determined from field measurements or calculated using the
56 thermodynamic model, our results reveal that the pH value of ambient organics-dominated
57 aerosols is sufficiently high to promote efficient SO₂ oxidation by NO₂ with NH₃ neutralization
58 under polluted conditions in China.

59

60

61 1. Introduction

62 Atmospheric measurements have demonstrated rapid sulfate production during severe haze
63 events in China (Guo et al., 2014; Wang et al., 2014; Zhang et al., 2015; Cheng et al., 2016;
64 Wang et al., 2016). For example, Wang et al. (2016) showed that during pollution episodes in
65 Xi'an of China the SO_4^{2-} mass concentration increased markedly from less than 10, 10-20, to
66 greater than $20 \mu\text{g m}^{-3}$, with the corresponding increases in the mean $\text{PM}_{2.5}$ mass concentrations
67 from 43, 139, to $250 \mu\text{g m}^{-3}$ from clean, transition, to polluted periods, respectively. Among the
68 $\text{PM}_{2.5}$ species in Xi'an, organic matter (OM), nitrate (NO_3^-), and SO_4^{2-} were most abundant, with
69 the mass fractions of 55%, 14%, and 14%, respectively, during the polluted period. In addition,
70 the work by Wang et al. (2016) demonstrated that the molar ratio of SO_4^{2-} to SO_2 , which reflects
71 sulfur partitioning between the particle and gas phases, exhibited an exponential increase with
72 relative humidity (RH), with the values of less than 0.1 at $\text{RH} < 20\%$ to 1.1 at $\text{RH} > 90\%$ in
73 Xi'an. Similar evolutions in SO_4^{2-} mass concentrations and the molar ratio of SO_4^{2-} to SO_2 were
74 shown during the pollution development in Beijing (Sun et al., 2013; Wang et al., 2014; Wang et
75 al., 2016). The rapid sulfate formation measured in China could not be explained by current
76 atmospheric models and suggested missing sulfur oxidation mechanisms (Wang et al., 2014).
77 Typically, high sulfate levels during haze events in China occurred concurrently with elevated
78 RH, NO_x , and NH_3 (Wang et al., 2014; Zhang et al., 2015; Wang et al., 2016), implicating an
79 aqueous sulfur oxidation pathway. On the basis of complementary field and experimental
80 measurements, Wang et al. (2016) concluded that the aqueous oxidation of SO_2 by NO_2 is key to
81 efficient sulfate formation, but is only feasible under two atmospheric conditions, i.e., on fine
82 aerosols with high RH and NH_3 neutralization or under cloud conditions.

83 Several recent studies estimated the particle acidity and aqueous sulfate production during

84 severe haze events in China using the thermodynamic model (Cheng et al., 2016; Guo et al.,
85 2017; Liu et al., 2017). For example, Cheng et al. (2016) estimated a pH range of 5.4 to 6.2 using
86 a thermodynamic model (ISORROPIA-II) in Beijing. On the basis of their estimated pH and the
87 previous experimental rates of SO₂ oxidation by NO₂ and the Henry's Law constants for sulfur
88 dioxide (SO₂), bisulfite (HSO₃⁻), and sulfite (SO₃²⁻) from the literature (Lee and Schwartz, 1983;
89 Clifton et al., 1988; Seinfeld and Pandis, 2006), the authors derived a sulfate production rate and
90 concluded that reactive nitrogen chemistry in aerosol water explained the sulfate formation
91 during polluted periods in Beijing. In contrast, other recent studies by Guo et al. (2017) and Liu
92 et al. (2017) adopted the similar method as Cheng et al. (2016), but reported significantly
93 different values of pH and the sulfate formation rates by the aqueous SO₂ oxidation by NO₂ in
94 China. Those two later studies determined a pH range of 3.0-4.9 and suggested that fine particles
95 were moderately acidic and the aqueous SO₂ oxidation by NO₂ was unimportant during severe
96 wintertime haze periods in China.

97 In this article, we conducted laboratory measurements of the hygroscopicity for oxalic acid
98 particles and particle growth of ammonium sulfate particles upon exposure to SO₂, NO₂, and
99 NH₃ at high RH conditions, in order to evaluate the dominant factors regulating the aqueous
100 oxidation of SO₂ by NO₂. In addition, field measurements of chemical compositions of water-
101 soluble fraction for fine PM (including oxalic acid) in Beijing, Hebei Province, and Xi'an of
102 China were performed during the winter haze episodes, showing significantly enriched water-
103 soluble organic matter (WSOM). The implications for the multi-aerosol chemical compositions
104 on the pH value and sulfate production during winter pollution periods in China are discussed.

105 **2. Methods**

106 **2.1 Aqueous phase oxidation of SO₂ by NO₂ in an environmental chamber**

107 The experimental method using the environmental chamber has been discussed elsewhere
108 (Wang et al., 2016), and here we only provide a brief description. The aqueous SO₂ oxidation
109 experiments was conducted by exposing size-selected (NH₄)₂SO₄ seed particles to different
110 levels of SO₂, NO₂, and NH₃ at variable RH conditions in a 1 m³ Teflon reaction chamber
111 covered with aluminum foil. A differential mobility analyzer (DMA) equipped with a
112 condensation particle counter (CPC) was used to measure the particle growth in diameter, in
113 order to determine sulfate formation on seeded particles (Wang et al., 2016).

114 **2.2 Measurement of hygroscopic growth factor of oxalic acid**

115 Hygroscopic growth factor (HGF) of oxalic acid was measured according to the method
116 previously discussed (Khalizov et al., 2009; Pagels et al., 2009). Briefly, a hygroscopicity
117 tandem differential mobility analyzer (HTDMA) coupled to a condensation particle counter
118 (CPC, TSI 3762) was used for the HGF measurement. Size-selected oxalic acid particles with the
119 dry diameter of 100 nm were exposed to increasing RH from 8% to 92% with a step range from
120 1%-10%. HGF is defined as the ratio of oxalic acid particle diameter (D_p) measured by the
121 second DMA at an elevated RH to the initial diameter ($D_0 = 100$ nm) of the particles selected by
122 the first DMA at the dry conditions of RH = 8% (Peng et al., 2016).

123 **2.3 Chemical composition of PM_{2.5} in Beijing, Hebei Province, and Xi'an, China**

124 PM_{2.5} samples were collected onto pre-baked (450°C for 6 hr) quartz fiber filter by using a
125 high-volume air sampler with an airflow rate of 1.03 m³ min⁻¹. The sample collection in Xi'an
126 was performed on the roof of a three-story building in the urban center with a 1-hour interval for
127 each sample during the winter of 2012 (Wang et al., 2016). The sample collection in Beijing was
128 conducted during the winter of 2016 on the roof of a four-story building on the campus of China
129 Research Academy of Environmental Sciences, which is located at the northern part of Beijing.

130 The PM_{2.5} samples in Hebei Province were collected during the winter of 2016 on the roof of a
131 three-story building on the campus of the Institute of Hydrology and Environmental Geology,
132 which is located in Zhengding County of Hebei Province. Both sample collections in Beijing and
133 Hebei Province were performed on a day/night basis. After collection, all samples were sealed
134 individually in an aluminum foil bag and stored in a freezer below -18°C prior to analysis.
135 During the sampling periods temperatures were -6.0 ± 4.0 °C (-15–1.0°C), -4.0 ± 3.0 °C (-
136 12–2.0°C) and 1.6 ± 4.4 °C (-5.4–15°C) in Beijing, Hebei Province and Xi’an, respectively, while
137 relative humidity at the three sites (RH) were $37 \pm 18\%$ (16–87%), $46 \pm 21\%$ (16–87%) and $59 \pm$
138 21% (15–95%), respectively. Previous observations showed that coal combustion, biomass
139 burnings and vehicle exhausts are the three major sources of PM_{2.5} during winter in North China
140 including Beijing, Hebei Province and Xi’an (Li et al., 2016; Zhang et al., 2015).

141 The detailed procedures for the analysis of inorganic ions and water-soluble organic matter
142 (WSOM) in aerosols have been reported elsewhere (Wang et al., 2009; Wang et al., 2010; Wang
143 et al., 2017). Briefly, one part of the filter sample (area about 5 cm²) was divided into several
144 pieces, extracted with Milli-Q pure water, and determined for WSOM and inorganic ions by
145 using Shimadzu TOC-L CPH analyzer and Dionex-600 ion chromatography, respectively.
146 Oxalic acid in PM_{2.5} was analyzed according to Wang et al. (2002) and Cheng et al. (2015). One
147 part of the filter sample was extracted with Milli-Q water, concentrated to dryness, and reacted
148 with 14% BF₃/butanol at 100°C for 1 hr. After the reaction, the derivatized sample was extracted
149 with hexane for three times and concentrated into 1 mL. Oxalic acid in the samples was
150 identified by gas chromatography–mass spectrometry (GC–MS) and quantified by gas
151 chromatography (Agilent GC7890A).

152 **3. Results**

153 3.1 Aqueous oxidation of SO₂ by NO₂ with NH₃ neutralization

154 We first evaluated the factors controlling the aqueous phase oxidation of SO₂ by NO₂ using
155 the environmental chamber method. The evolution in the size of ammonium sulfate particles
156 after exposure to SO₂, NO₂, and NH₃ at different RH and SO₂ levels is shown in Figure 1. In our
157 experiments, monodisperse particles with the initial dry particle size ranging from 50 to 70 nm
158 were selected for the exposure, and two different SO₂ concentrations (37.5 and 375 parts per
159 billions or ppb) were used. RH was maintained at a level of 80-98%, above the deliquescence
160 point (79%) of ammonium sulfate (Qiu and Zhang, 2013) to ensure aqueous particles. As is
161 shown in Figure 1, the size of (NH₄)₂SO₄ particles remains nearly invariant (within the
162 experimental uncertainty) after exposure to SO₂, NO₂, and NH₃. A 10-fold increase in the SO₂
163 concentration has little effect on the growth of (NH₄)₂SO₄ particles. These results illustrate that
164 sulfate production is insignificant and SO₂ cannot be efficiently oxidized by NO₂ in the presence
165 of NH₃ on aqueous ammonium sulfate particles. The measurement of negligible growth for
166 (NH₄)₂SO₄ particles exposed to SO₂, NO₂, and NH₃ at high RH is in contrast to the previous
167 work by Wang et al. (2016), which showed large size growth and significant sulfate production
168 for oxalic acid particles with NH₃ neutralization and under high RH conditions (see the black
169 triangles in Figure 1).

170 To gain an insight into such a difference in the size growth between (NH₄)₂SO₄ and oxalic
171 acid particles, we measured the hygroscopic growth of oxalic acid particles. Figure 2 displays the
172 measured hygroscopic growth factor (HGF) of oxalic acid, showing an exponential increase with
173 an increase in RH. The measured HGF value is close to unity at RH < 40% and increases from
174 1.1 at RH = 60% to 1.5 at RH = 90%. Our measured HGF for oxalic acid is consistent with the
175 previous studies by Prenni et al. (2001) and Mikhailov et al. (2009); all of which were measured

176 by using a hygroscopicity tandem differential mobility analyzer (HTDMA) system. On the other
177 hand, another earlier experimental study showed little growth for oxalic acid particles under high
178 RH conditions by using an electrodynamic balance (EDB) system (Peng et al., 2001). The
179 different HGF measured for oxalic acid is most likely due to the different accuracies of the two
180 types of methods for the hygroscopicity measurement. The measurements of HGF also provide
181 information on the particle phase-state. As evident from Figure 2, oxalic acid particles mainly
182 exist in a non-aqueous phase at $RH < 40\%$ but in the aqueous phase at $RH > 60\%$.

183 Our present experiments of aqueous oxidation of SO_2 by NO_2 were performed at similar
184 conditions as those by Wang et al. (2016), i.e., with comparable concentrations for SO_2 , NO_2 ,
185 and NH_3 and in the same phase-state (aqueous) for the particles. On the other hand, the particle
186 acidity is clearly distinct between the two studies. Our present experiment is characterized by a
187 lower pH value, since ammonium sulfate is rather acidic. For example, the pH value of 0.1M
188 $(NH_4)_2SO_4$ solution is 5.5. The overall aqueous reaction between SO_2 and NO_2 in the presence of
189 NH_3 is suggested as the following (Wang et al., 2016),



191 Since the solubility of SO_2 decreases markedly with increasing particle acidity (Seinfeld and
192 Pandis, 2006; Zhang et al., 2015), the heterogeneous reaction between SO_2 and NO_2 is prohibited
193 on acidic $(NH_4)_2SO_4$ particles. On the other hand, under the experimental conditions by Wang et
194 al. (2016), the heterogeneous reaction between oxalic acid and NH_3 occurred on aqueous
195 particles in the presence of NH_3 , yielding ammonium oxalate. The ammonium oxalate is
196 expected to be less acidic than ammonium sulfate, because for a bulk solution the pH value of
197 0.1 M ammonium oxalate is 6.5 and one unit higher than that of ammonium sulfate. As a result,
198 SO_2 readily dissolves into aqueous ammonium oxalate particles and is oxidized by NO_2 into

199 SO_4^{2-} , which is consequently neutralized by NH_3 to produce $(\text{NH}_4)_2\text{SO}_4$. The resulting aqueous
200 ammonium oxalate/ $(\text{NH}_4)_2\text{SO}_4$ particles, which is internally mixed, exhibit a lower acidity than
201 that of pure $(\text{NH}_4)_2\text{SO}_4$ particles, responsible for a significant growth in the dry particle size and
202 sulfate formation for the previous experiments by Wang et al. (2016).

203 Hence, the experimental studies of our present work and that by Wang et al. (2016) reveal
204 that sulfate production on fine particles is dependent on several factors, including the particle
205 hygroscopicity, phase-state, acidity, and RH, in addition to the gaseous concentrations of SO_2 ,
206 NO_2 , and NH_3 . These experimental results indicate that the acidity and sulfate formation are
207 distinct for organic seed and ammonium sulfate seed particles. While oxidation of SO_2 by NO_2
208 on aqueous $(\text{NH}_4)_2\text{SO}_4$ particles does not represent a viable mechanism because of a higher
209 acidity, significant sulfate production occurs on oxalic acid particles because of a lower acidity.

210 **3.2 Field measurements of WSOM in China**

211 Atmospheric measurements have shown that the occurrence of severe haze episodes in
212 China is accompanied with high RH conditions and $\text{PM}_{2.5}$ particles consist of large amounts of
213 secondary organic and inorganic compounds. We present additional field measurements of the
214 chemical composition of $\text{PM}_{2.5}$ in Beijing, Hebei Province, and Xi'an of China. Figure 3 shows
215 that the wintertime $\text{PM}_{2.5}$ samples collected at the three locations. It is evident that WSOM is
216 considerably enriched and their concentrations are comparable to those of the total inorganic ions
217 (Figure 3a and b). For example, the mass concentration of WSOM ranges from 10 to $60 \mu\text{g m}^{-3}$
218 in Beijing and Hebei Province during the winter of 2016 and from 10 to $180 \mu\text{g m}^{-3}$ in Xi'an
219 during the winter of 2012 (Figure 3c and d, respectively). Compared to those in Beijing and
220 Hebei Province, the more abundant WSOM in Xi'an was caused by more emissions from
221 biomass burning for house heating (Li et al., 2016). As seen in Figure 3c–f, the variation of

222 WSOM displays a temporal pattern similar to that of oxalic acid, with a linear correlation
223 coefficient of 0.79, 0.88 and 0.72 in Beijing, Hebei Province, and Xi'an, respectively (Figure 3e
224 and f). The mass concentration of oxalic acid in fine PM during the haze episodes is about 500
225 ng m^{-3} in Beijing and Hebei Province (Figure 3e) and more than 2000 ng m^{-3} in Xi'an (Figure 3f).
226 Hence, our field measurements indicate that oxalic acid represents one of the most abundant
227 WSOM in the aerosol-phase. Oxalic acid is a secondary product formed from the aqueous-phase
228 oxidation of water-soluble organic precursors and ubiquitously exists in the troposphere. Like
229 other pollutants, oxalic acid has been also shown to occur with large abundance in China (Wang
230 et al., 2012; Cheng et al., 2013; Meng et al., 2014; Kawamura and Bikkina, 2016). As shown in
231 Figure 3g and h, during the field observation periods sulfate at the three sites showed a temporal
232 variation pattern similar to that of oxalic acid with a robust linear correlation ($r^2=0.67, 0.84$ and
233 0.61 in Xi'an, Beijing and Hebei Province, respectively). Such a correlation was also reported by
234 other researchers (Wang et al, 2017, Yu et al, 2005), suggesting the cooccurrence and internally
235 mixing state of both compounds in the atmosphere. In addition, the previous field measurements
236 also revealed that WSOM in China is not only enriched in carboxylic acids (including oxalic acid)
237 but also in other organic species, including carbonyls, amines, and water-soluble nitrogen-
238 containing organic compounds (Wang et al., 2010, 2013; Zheng et al., 2015; Yao et al., 2016;
239 Liu et al., 2017). The dominant organic acids and bases indicate that haze particles in China are
240 multi-component in nature and the estimations of the particle acidity (or pH) and the sulfate
241 production rate need to take into account of the effects of organic species, in addition to
242 inorganic ions.

243 **4. Discussions**

244 Several recent studies using the thermodynamic models (Wexler and Clegg, 2002;

245 Fountoukis and Nenes, 2007) estimated the particle acidity and sulfate production during
246 pollution episodes in China (Cheng et al., 2016; Guo et al., 2017; Liu et al., 2017). Those
247 previous studies treated the PM exclusively as a mixture of inorganic salts dominated by
248 ammonium sulfate and neglected the effects due to the presence of organic compounds.
249 Apparently, the conclusions by those modeling studies hinge on the validity of several critical
250 assumptions in their analyses, including the application of the thermodynamic model, the
251 accuracy in determining the aerosol water content (AWC), and the applicability of the earlier
252 experimental measurements for the aqueous oxidation of SO₂ by NO₂ to atmospheric conditions.

253 Estimation of the pH values using the thermodynamic models is typically of considerable
254 uncertainty, because of several intricate difficulties. For example, the ISORRPIA-II model
255 includes two modes, i.e., metastable (aerosols are assumed to be in the liquid-phase only and
256 may reach supersaturation) and stable (aerosols are assumed in the liquid- and solid phases that
257 are in equilibrium) (Guo et al., 2017). Since the thermodynamic model is established on the basis
258 of the equilibrium principles, its application to non-equilibrium conditions needs to be rigorously
259 assessed. Also, the phase (e.g., liquid, amorphous, or crystalline) and mixing state of ambient
260 aerosols are highly complex because of the presence of multi-component organic and inorganic
261 species (Qiu and Zhang, 2013; Zhang et al., 2015), inevitably rendering high uncertainty in the
262 thermodynamic calculations.

263 Guo et al. (2017) suggested that the pH predictions using the metastable mode would be
264 more reliable than that using the stable mode, on the basis of model evaluation from measured
265 and predicted NO₃⁻ and NH₄⁺ during the winter of 2012 in Xi'an. Figure 4 compares the
266 concentrations of NH₃ (g) and aerosol species predicted by ISORROPIA-II with the field
267 measurements under the metastable and stable modes in Xi'an during the winter of 2012. As

268 evident in Figure 4a and b, NH_3 predicted is similar to the measured value with the metastable or
269 stable mode. Furthermore, the predicted concentrations of NO_3^- and NH_4^+ using both the
270 metastable and stable modes are nearly identical (Fig. 4c-f). Guo et al. (2017) only compared the
271 liquid NH_4^+ and NO_3^- predicted by the model under the stable mode with the field measured
272 aerosols composed of both liquid and solid compounds, and thus their predicted concentrations
273 were lower than those of the measurements (see Figure S1 in Guo et al, 2017). As a result, their
274 statement that pH prediction with the metastable mode would be more reliable than that with the
275 stable mode was unjustified. Noticeably, the pH values estimated by the ISORROPIA-II model
276 under the two modes are significantly different, with the values of 4.57 ± 0.40 under the
277 metastable mode and 6.96 ± 1.33 under the stable mode. Most recently, it was suggested that the
278 large discrepancy in predicting pH is attributable to the model code errors (Song et al., 2018).

279 In addition, the pH estimation by the thermodynamic model is highly dependent on the ratio
280 of the concentration of hydrogen ions in the liquid-phase to AWC. Guo et al. (2017) and Liu et al.
281 (2017) assumed negligible particle water associated with the organic aerosol mass. Such an
282 assumption is clearly invalid since aerosols typically contain a large portion of WSOM in China
283 (Fig. 3), including organic nitrogen species (Wang et al., 2010, 2013) and acids (Wang et al.,
284 2006, 2009, 2010). Also, organic acids engage in particle-phase reactions with the basic species
285 (i.e., NH_3 and amines), significantly enhancing the particle hygroscopicity and reducing the
286 acidity (Gomez-Hernandez et al., 2016). In addition, because of their strong basicity and high
287 abundance, amines likely play a key role in reducing the particle-acidity in China (Wang et al.,
288 2010a, b; Qiu et al., 2011; Qiu and Zhang, 2012; Dong et al., 2013; Zheng et al., 2015; Yao et al.,
289 2016; Liu et al., 2017). Consequently, the acidity for organics-dominated aerosols is
290 considerably different from that of ammonium sulfate aerosols, as demonstrated in our

291 experimental results. While effort has been made to account for the effects of organic species on
292 the aerosol properties (Clegg et al., 2013), the available thermodynamic models are still
293 inadequate in representing complex multi-component aerosols. An inconsistency of the
294 ammonium–sulfate ratios using the thermodynamic models was identified in the eastern US, also
295 suggesting a possible role for organic species (Silvern et al., 2017).

296 Furthermore, the chemical mechanism leading to the aqueous conversion of SO₂ to sulfate
297 by NO₂ is not well understood. The previous modeling studies adopted the aqueous reaction rate
298 constants previously measured (Lee and Schwartz, 1983; Clifton et al., 1988), while the
299 applicability of the earlier experimental studies to atmospheric conditions is uncertain. For
300 example, Lee and Schwartz (1983) examined the oxidation of S(IV) by NO₂ in the liquid phase
301 by flowing gaseous NO₂ through a NaHSO₃ solution at a constant pH by regulating NaOH and
302 determined the rate constant of $1.4 \times 10^5 \text{ M}^{-1} \text{ s}^{-1}$ at pH = 5 and with a lower limit of $2 \times 10^6 \text{ M}^{-1} \text{ s}^{-1}$
303 ¹ at pH = 5.8 and 6.4 from measuring the electrical conductivity of the solution. Clifton et al.
304 (1988) measured the rate constant for the reaction of NO₂ with S(IV) over the pH range of 5.3-13,
305 by producing NO₂ from irradiation of NaNO₂ and N₂O solutions and mixing with Na₂SO₃
306 solutions, and obtained the second-order rate constant of 1.24×10^7 and $2.95 \times 10^7 \text{ M}^{-1} \text{ s}^{-1}$ from
307 the decay of NO₂ monitored by absorption spectroscopy. The results of the measured rate
308 constants between the two earlier experimental measurements differed by 1-2 orders of
309 magnitude (Lee and Schwartz, 1983; Clifton et al., 1988). Also, both kinetic experiments
310 employed bulk solutions and did not account for the gaseous uptake process (Lee and Schwartz,
311 1983; Clifton et al., 1988).

312 Wang et al. (2016) obtained the SO₂ uptake coefficient for sulfate production from
313 combined field measurements and laboratory experiments, and their laboratory experiments

314 using aqueous oxalic acid particles reproduced the rapid sulfate production measured under
315 polluted ambient conditions in China. The SO₂ uptake coefficient on oxalic acid particles in the
316 laboratory reaction chamber is $8.3 \pm 5.7 \times 10^{-5}$ (Wang et al., 2016) under the humid conditions and
317 similar to that ($4.5 \pm 1.1 \times 10^{-5}$) (Wang et al., 2016) observed in Beijing during the haze period of
318 2015. The results of the SO₂ uptake coefficients determined by Wang et al. (2016) are also
319 consistent with the modeling studies in quantification of the sulfate formation using atmospheric
320 models in the country (e.g., Wang et al., 2014), indicating the applicability of their proposed
321 mechanism to haze conditions in China. On the other hand, Liu et al. (2017) invoked the
322 experimental work by Hung et al. (2015) as a plausible cause for rapid SO₂ oxidation by O₂ in
323 the absence of photochemistry, but without noting the high acidity as a necessary condition in
324 that experimental work (i.e., pH \leq 3). Most recently, Li et al. (2018) suggested an indirect
325 mechanism of SO₂ oxidation by NO₂ via HONO/NO₂⁻ produced in fast-hydrolytic
326 disproportionation of NO₂ on the surface of NaHSO₃ aqueous microjets. In addition, another
327 recent theoretical work by Zhang et al. (2018) indicated that under weakly acidic and neutral
328 conditions (pH \leq 7) the oxidation of HOSO₂⁻ by dissolved NO₂ is a self-sustaining process,
329 where the produced *cis*-HONO, HSO₄⁻ and H₂SO₄ promote the tautomerization from HSO₃⁻ to
330 HOSO₂⁻ as the catalysts.

331 **5. Conclusions**

332 In this paper we have presented experimental measurements of the growth of ammonium
333 sulfate seed particles exposed to vapors of SO₂, NO₂, and NH₃ at variable RH, the HGF of oxalic
334 acid particles, and field measurements of WSOM for PM_{2.5} during the severe haze events in
335 Beijing, Hebei Province, and Xi'an of China. Our experimental results reveal that sulfate
336 production on fine particles is dependent on the particle hygroscopicity, phase-state, and acidity,

337 as well as RH. The acidity and sulfate formation for ammonium sulfate seed particles are distinct
338 from those of oxalic acid seed particles. Aqueous ammonium sulfate particles show negligible
339 growth because of low pH, in contrast to aqueous oxalic acid particles with significant dry-size
340 increase and sulfate formation because of high pH. In addition, our atmospheric measurements
341 show significant concentrations of WSOM (including oxalic acid) in fine PM, indicating multi-
342 component haze particles in China. Our results reveal that a particle mixture of inorganic salts
343 adopted by the previous studies using the thermodynamic model does not represent a suitable
344 model system and that the particle acidity and aqueous sulfate formation rate cannot be reliably
345 inferred without accounting for the effects of multi-chemical compositions during severe haze
346 events in China. Our combined experimental and field measurements corroborate the earlier
347 finding that sulfate production via the particle-phase reaction involving SO_2 and NO_2 with NH_3
348 neutralization occurs efficiently on organics-dominated aerosols (Wang et al., 2016) but are in
349 contradiction to the most recent studies using the thermodynamic model (Guo et al., 2017; Liu et
350 al., 2017).

351 In conclusion, while the particle acidity or pH cannot be accurately determined from
352 atmospheric field measurements or calculated using the thermodynamic models, our combined
353 experimental and field results provide the compelling evidence that the pH value of ambient
354 organics-dominated particles is sufficiently high to promote SO_2 oxidation by NO_2 with NH_3
355 neutralization under polluted conditions in China.

356 **Acknowledgements**

357 Financial support for this work was provided by National Key R&D Plan (Quantitative
358 Relationship and Regulation Principle between Regional Oxidation Capacity of Atmospheric and
359 Air Quality (No. 2017YFC0210000), the China National Natural Science Funds for

360 Distinguished Young Scholars (No.41325014), the program from National Nature Science
361 Foundation of China (No. 41773117). This work was also supported by the Robert A. Welch
362 Foundation (Grant A-1417) W.M.-O. was supported by the National Science Foundation
363 Graduate Research Fellowship Program.

364

365 **References**

- 366 Cheng, C., Wang, G., Zhou, B., Meng, J., Li, J., Cao, J., and Xiao, S.: Comparison of
367 dicarboxylic acids and related compounds in aerosol samples collected in Xi'an, China
368 during haze and clean periods, *Atmospheric Environment*, 81(0), 443-449, 2013.
- 369 Cheng, C., Wang, G., Meng, J., Wang, Q., Cao, J., Li, J., and Wang, J.: Size-resolved airborne
370 particulate oxalic and related secondary organic aerosol species in the urban atmosphere of
371 Chengdu, China, *Atmospheric Research*, 161–162, 134-142, 2015.
- 372 Cheng, Y., Zheng, G., Wei, C., Mu, Q., Bo Zheng, Wang, Z., Gao, M., Zhang, Q., He, K.,
373 Carmichael, G., Pöschl, U., and Su, H.: Reactive nitrogen chemistry in aerosol water as a
374 source of sulfate during haze events in China, *Science Advances*, 2, e1601530, 2016.
- 375 Clegg, S.L., Qiu, C., Zhang, R.: The deliquescence behaviour, solubilities, and densities of
376 aqueous solutions of five methyl- and ethyl-aminium sulphate salts, *Atmospheric
377 Environment*, 73, 1-14, 2013.
- 378 Clifton, C. L., Altstein, N., and Huie, R. E.: Rate constant for the reaction of nitrogen dioxide
379 with sulfur(IV) over the pH range 5.3-13, *Environmental Science & Technology*, 22, 586-
380 589, 1988.
- 381 Dong, X. L., Liu, D. M., and Gao, S. P.: Seasonal variations of atmospheric heterocyclic
382 aromatic amines in Beijing, China, *Atmospheric Research*, 120, 287-297, 2013.
- 383 Fountoukis, C., and Nenes, A.: ISORROPIA II: A computationally efficient thermodynamic
384 equilibrium model for K^+ - Ca^{2+} - Mg^{2+} - NH_4^+ - Na^+ - SO_4^{2-} - NO_3^- - Cl^- - H_2O aerosols, *Atmospheric
385 Chemistry and Physics*, 7, 4639-4659, 2007.
- 386 Gomez-Hernandez, M., McKeown, M., Secret, J., Marrero-Ortiz, W., Lavi, A., Rudich, Y.,
387 Collins, D. R., and Zhang, R.: Hygroscopic characteristics of alkylammonium carboxylate
388 Aerosols, *Environmental Science & Technology*, 50, 2292-2300, 2016.
- 389 Guo, H., Weber, R. J., and Nenes, A.: High levels of ammonia do not raise fine particle pH
390 sufficiently to yield nitrogen oxide-dominated sulfate production, *Scientific Reports*, 7,
391 12109, doi:12110.11038/s41598-12017-11704-12100, 2017.
- 392 Guo, H., Liu, J., Froyd, K. D., Roberts, J. M., Veres, P. R., Hayes, P. L., Jimenez, J. L., Nenes,
393 A., and Weber, R. J.: Fine particle pH and gas–particle phase partitioning of inorganic
394 species in Pasadena, California, during the 2010 CalNex campaign, *Atmospheric Chemistry
395 and Physics*, 17, 5703-5719, 2017.
- 396 Guo, S., Hu, M., Zamora, M. L., Peng, J. F., Shang, D. J., Zheng, J., Du, Z. F., Wu, Z., Shao, M.,
397 Zeng, L. M., Molina, M. J., and Zhang, R. Y.: Elucidating severe urban haze formation in
398 China, *Proceedings of the National Academy of Sciences of the United States of America*,
399 111, 17373-17378, 2014.
- 400 Hung, H.-M., and Hoffman, M. R.: Oxidation of gas-phase SO₂ on the surfaces of acidic
401 microdroplets: Implications for sulfate and sulfate radical anion formation in the
402 atmospheric liquid phase, *Environmental Science & Technology*, 49, 13768-13776, 2015.
- 403 Kawamura, K., and Bikina, S.: A review of dicarboxylic acids and related compounds in
404 atmospheric aerosols: Molecular distributions, sources and transformation, *Atmospheric
405 Research*, 170, 140-160, 2016.
- 406 Khalizov, A.F., Zhang, R., Zhang, D. Xue, H., Pagels, J., and McMurry, P.H.: Formation of
407 highly hygroscopic aerosols upon internal mixing of airborne soot particles with sulfuric
408 acid vapor, *Journal of Geophysical Research-Atmospheres*, 114, D05208,
409 doi:10.1029/2008JD010595, 2009.

410 Lee, Y. N., and Schwartz, S. E.: Kinetics of oxidation of aqueous sulfur (IV) by nitrogen
411 dioxide, in Precipitation scavenging, dry deposition, and resuspension, edited by H. R.
412 Pruppacher, R. G. Semmon and W. G. N. Slinm, Elsevier, New York, 1983.

413 Li, J., Wang, G., Ren, Y., Wang, J., Wu, C., Han, Y., Zhang, L., Cheng, C., and Meng, J.:
414 Identification of chemical compositions and sources of atmospheric aerosols in Xi'an, inland
415 China during two types of haze events, *Science of the Total Environment*, 566-567, 230-237,
416 2016..

417 Li, L., Hoffmann, M. R., and Colussi, A. J.: The role of nitrogen dioxide in the production of
418 sulfate during Chinese haze-aerosol episodes, *Environmental Science & Technology* 52,
419 DOI: 10.1021/acs.est.7b05222, 2018.

420 Liu, F., Bi, X., Zhang, G., Peng, L., Lian, X., Lu, H., Fu, Y., Wang, X., Peng, P. a., and Sheng,
421 G.: Concentration, size distribution and dry deposition of amines in atmospheric particles of
422 urban Guangzhou, China, *Atmospheric Environment*, 171, 279-288, 2017.

423 Liu, M., Song, Y., Zhou, T., Xu, Z., Yan, C., Zheng, M., Wu, Z., Hu, M., Wu, Y., and Zhu, T.:
424 Fine particle pH during severe haze episodes in Northern China, *Geophysical Research*
425 *Letters*, 44, 5213-5221 ,doi: 5210.1002/2017GL073210, 2017.

426 Meng, J., Wang, G., Li, J., Cheng, C., Ren, Y., Huang, Y., Cheng, Y., Cao, J., and Zhang, T.:
427 Seasonal characteristics of oxalic acid and related SOA in the free troposphere of Mt. Hua,
428 central China: Implications for sources and formation mechanisms, *Science of the Total*
429 *Environment*, 493, 1088-1097, 2014.

430 Mikhailov, E., Vlasenko, S., Martin, S. T., Koop, T., and Poeschl, U.: Amorphous and crystalline
431 aerosol particles interacting with water vapor: conceptual framework and experimental
432 evidence for restructuring, phase transitions and kinetic limitations, *Atmospheric Chemistry*
433 *and Physics*, 9, 9491-9522, 2009.

434 Pagels, J., McMurry, P.H., Khalizov, A.F., and Zhang, R.: Processing of soot by controlled
435 sulphuric acid and water condensation—Mass and mobility relationship, *Aerosol Science &*
436 *Technology*, 43, 629–640, 2009.

437 Peng, J., Hu, M., Guo, S., Du, Z., Zheng, J., Shang, D., Zamora, M.L., Zeng, L., Shao, M., Wu,
438 Y., Zheng, J., Wang, Y., Glen, C.R., Collins, D.R., Molina, M.J., and Zhang, R.: Markedly
439 enhanced absorption and direct radiative forcing of black carbon under polluted urban
440 environments, *Proceedings of the National Academy of Sciences of the United States of*
441 *America*, 113, 4266–4271, 2016.

442 Peng, C., Chan, M. N., and Chan, C. K.: The hygroscopic properties of dicarboxylic and
443 multifunctional acids: measurements and UNIFAC predictions, *Environmental Science &*
444 *Technology*, 35, 4495-4501, 2001.

445 Prenni, A. J., DeMott, P. J., Kreidenweis, S. M., Sherman, D. E., Russell, L. M., and Ming, Y.:
446 The effects of low molecular weight dicarboxylic acids on cloud formation, *Journal of*
447 *Physical Chemistry A*, 105, 11240-11248, 2001.

448 Qiu, Q., Wang, L., Lal, V., Khalizov, A.F., and Zhang, R.: Heterogeneous chemistry of
449 Alkylamines on Ammonium Sulfate and Ammonium Bisulfate, *Environmental Science &*
450 *Technology*, 45, 4748–4755, 2011.

451 Qiu, C., and Zhang, R.: Physiochemical Properties of Alkylaminium Sulfates: Hygroscopicity,
452 Thermostability, and Density, *Environmental Science & Technology*, 46, 4474-4480, 2012.

453 Qiu, C., and Zhang, R. Y.: Multiphase chemistry of atmospheric amines, *Physical Chemistry*
454 *Chemical Physics*, 15(16), 5738-5752, 2013.

455 Seinfeld, J. H., and Pandis, S. N., *Atmospheric Chemistry and Physics: From Air Pollution to*

456 *Climate Change, 2nd ed.*, John Wiley & Sons, Hoboken, NJ, 2006.

457 Silvern, R.F., Jacob, D.J., Kim, P.S., Marais, E.A., Turner, J. R., Campuzano-Jost, P., and

458 Jimenez, J. L. Inconsistency of ammonium–sulfate aerosol ratios with thermodynamic

459 models in the eastern US: a possible role of organic aerosol, *Atmospheric Chemistry and*

460 *Physics*, 17, 5107–5118, 2017.

461 Song, S., Gao, M., Xu, W., Shao, J., Shi, G., Wang, S., Wang, Y., Sun, Y., and McElroy, M. B.:

462 Fine particle pH for Beijing winter haze as inferred from different thermodynamic

463 equilibrium models, *Atmospheric Chemistry and Physics Discussions*,

464 <https://doi.org/10.5194/acp-2018-6>, 2018.

465 Sun, Y. L., Wang, Z. F., Fu, P. Q., Yang, T., Jiang, Q., Dong, H. B., Li, J., and Jia, J. J.: Aerosol

466 composition, sources and processes during wintertime in Beijing, China, *Atmospheric*

467 *Chemistry and Physics*, 13(9), 4577-4592, 2013.

468 Wang, G., Xie, M., Hu, S., Tachibana, E., and Kawamura, K.: Dicarboxylic acids, metals and

469 isotopic compositions of C and N in atmospheric aerosols from inland China: Implications

470 for dust and coal burning emission and secondary aerosol formation, *Atmospheric*

471 *Chemistry and Physics*, 10, 6087-6096, 2010.

472 Wang, G., Kawamura, K., Umemoto, N., Xie, M., Hu, S., and Wang, Z.: Water-soluble organic

473 compounds in PM_{2.5} and size-segregated aerosols over Mt. Tai in North China Plain,

474 *Journal of Geophysical Research-Atmospheres*, 114, D19208,

475 [doi:10.1029/2008JD011390](https://doi.org/10.1029/2008JD011390), 2009.

476 Wang, G., Kawamura, K., Cao, J., Zhang, R., Cheng, C., Li, J., Zhang, T., Liu, S., and Zhao, Z.:

477 Molecular distribution and stable carbon isotopic composition of dicarboxylic acids,

478 ketocarboxylic acids and α -dicarbonyls in size-resolved atmospheric particles from Xi'an

479 city, China, *Environmental Science & Technology*, 46, 4783-4791, 2012.

480 Wang, G., Zhang, R., Zamora, M. L., Gomez, M. E., Yang, L., Hu, M., Lin, Y., Guo, S., Meng,

481 J., Li, J., Cheng, C., Hu, T., Ren, Y., Wang, Y., Gao, J., Cao, J., An, Z., Zhou, W., Wang, J.,

482 Marrero-Ortiz, W., Tian, P., Secrest, J., Peng, J., Du, Z., Zheng, J., Shang, D., Zeng, L.,

483 Shao, M., Wang, W., Huang, Y., Wang, Y., Zhu, Y., Li, Y., Hu, J., Pan, B., Cai, L., Cheng,

484 Y., Rosenfeld, D., Liss, P. S., Duce, R. A., Kolb, C. E., and Molina, M. J.: Persistent Sulfate

485 Formation from London Fog to Chinese Haze, *Proceedings of National Academy of Science*

486 *of United States of America*, 113(48), 13630-13635, [doi/10.1073/pnas.1616540113](https://doi.org/10.1073/pnas.1616540113),

487 2016.

488 Wang, G. H., Niu, S. L., Liu, C., and Wang, L. S.: Identification of dicarboxylic acids and

489 aldehydes of PM₁₀ and PM_{2.5} aerosols in Nanjing, China, *Atmospheric Environment*,

490 36(12), 1941-1950, 2002.

491 Wang, G. H., Kawamura, K., Watanabe, T., Lee, S. C., Ho, K. F., and Cao, J. J.: Heavy loadings

492 and source strengths of organic aerosols in China, *Geophysical Research Letters*, 33,

493 L22801, [doi:10.1029/2006GL027624](https://doi.org/10.1029/2006GL027624), 2006.

494 Wang, G. H., Zhou, B. H., Cheng, C. L., Cao, J. J., Li, J. J., Meng, J. J., Tao, J., Zhang, R. J., and

495 Fu, P. Q.: Impact of Gobi desert dust on aerosol chemistry of Xi'an, inland China during

496 spring 2009: differences in composition and size distribution between the urban ground

497 surface and the mountain atmosphere, *Atmospheric Chemistry and Physics*, 13(2), 819-835,

498 2013.

499 Wang, J., Wang, G., Gao, J., Wang, H., Ren, Y., Li, J., Zhou, B., Wu, C., Zhang, L., Wang, S.,

500 and Chai, F.: Concentrations and stable carbon isotope compositions of oxalic acid and

501 related SOA in Beijing before, during, and after the 2014 APEC, *Atmospheric Chemistry*

502 and Physics, 17(2), 981-992, 2017.

503 Wang, L., Lal, V., Khalizov, A.F., and Zhang, R.: Heterogeneous chemistry of alkylamines with
504 sulfuric acid: Implications for atmospheric formation of alkylammonium sulfates,
505 Environmental Science & Technology, 44, 2461–2465, 2010a.

506 Wang, L., Khalizov, A.F., Zheng, J., Xu, W., Lal, V., Ma, Y., and Zhang, R.: Atmospheric
507 nanoparticles formed from heterogeneous reactions of organics, Nature Geoscience, 3, 238-
508 242, 2010b.

509 Wang, Y., Zhang, Q., Jiang, J., Zhou, W., Wang, B., He, K., Duan, F., Zhan, Q., Philip, S., and
510 Xie, Y.: Enhanced sulfate formation during China's severe winter haze episode in January
511 2013 missing from current models, Journal Geophysical Research-Atmospheres, 119(17),
512 10425-10440, doi:10.1002/12013JD021426, 2014.

513 Wexler, A.S., and Clegg, S. L.: Atmospheric aerosol models for systems including the ions H^+ ,
514 NH_4^+ , Na^+ , SO_4^{2-} , NO_3^- , Cl^- , Br^- and H_2O . Journal of Geophysical Research, 107 (D14),
515 4207, doi:10.1029/2001JD000451, 2002.

516 Yao, L., Wang, M.-Y., Wang, X.-K., Liu, Y.-J., Chen, H.-F., Zheng, J., Nie, W., Ding, A.-J.,
517 Geng, F.-H., Wang, D.-F., Chen, J.-M., Worsnop, D. R., and Wang, L.: Detection of
518 atmospheric gaseous amines and amides by a high-resolution time-of-flight chemical
519 ionization mass spectrometer with protonated ethanol reagent ions, Atmospheric Chemistry
520 and Physics, 16(22), 14527-14543, 2016.

521 Yu, J. Z., Huang, X. F., Xu, J. H., and Hu, M.: When aerosol sulfate goes up, so does oxalate:
522 Implication for the formation mechanisms of oxalate, Environmental Science & Technology,
523 39(1), 128-133, 2005.

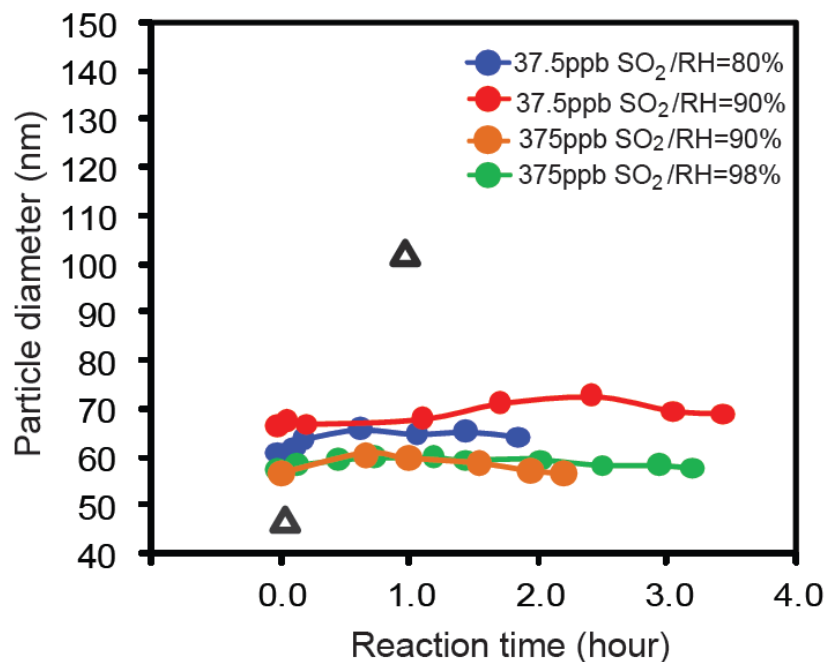
524 Zhang, R., Wang, G., Guo, S., Zamora, M. L., Ying, Q., Lin, Y., Wang, W., Hu, M., and Wang,
525 Y.: Formation of urban fine particulate matter, Chemical Reviews, 115, 3803-3855,
526 doi:10.1021/acs.chemrev.3805b00067, 2015.

527 Zhang, H., Chen, S., Zhong, J., Zhang, S., Zhang, Y., Zhang, X., Li, Z., and Zeng, X.C.:
528 Formation of aqueous-phase sulfate during the haze period in China: Kinetics and
529 atmospheric implications, Atmospheric Environment, 177, 93-99, 2018.

530 Zheng, J., Ma, Y., Chen, M., Zhang, Q., Wang, L., Khalizov, A. F., Yao, L., Wang, Z., Wang, X.,
531 and Chen, L.: Measurement of atmospheric amines and ammonia using the high resolution
532 time-of-flight chemical ionization mass spectrometry, Atmospheric Environment, 102, 249-
533 259, 2015.

534
535
536

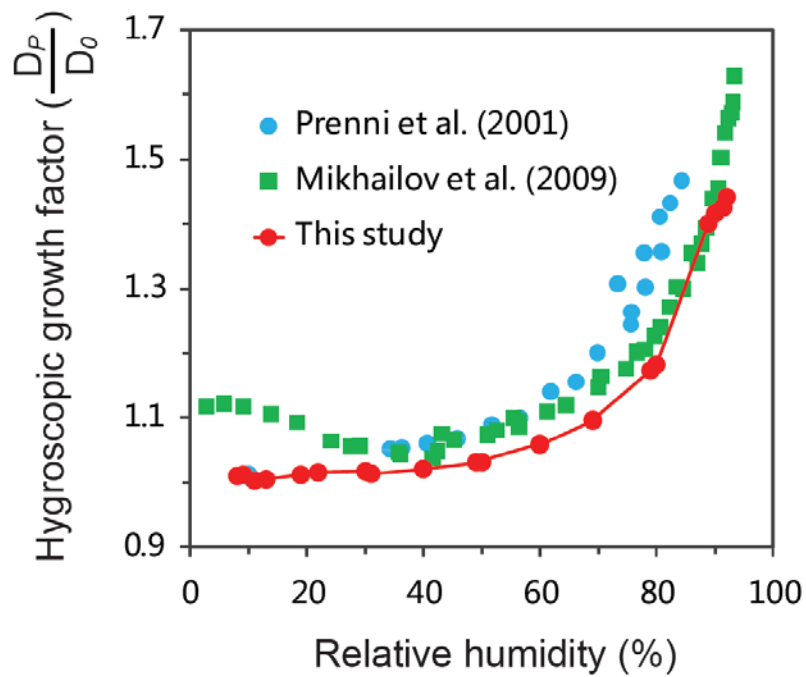
537
538



539
540
541
542
543
544
545
546
547
548
549
550
551

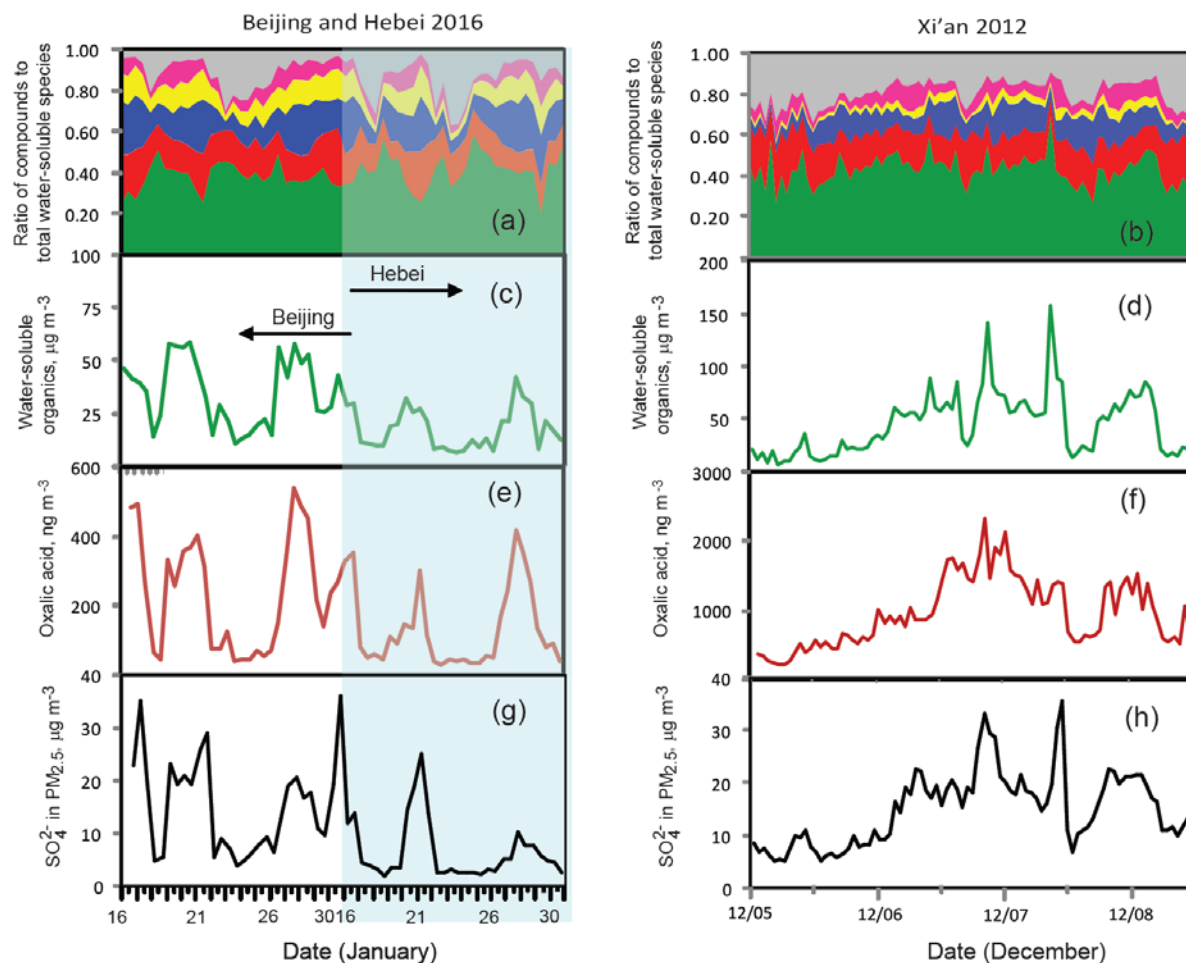
Figure 1. Size evolution of ammonium sulfate (circle dots) and oxalic acid (black triangles) particles after exposure to SO₂, NO₂, and NH₃ at different RH levels. Variations in mobility diameter (D_p) of the particles as a function of reaction time. The symbols with different colors denote measurements with exposure to different SO₂, NO₂ and NH₃ concentrations and RH levels. For the ammonium sulfate particles exposure experiment, two levels of SO₂ were used, which are 37.5 ppb and 375 ppb, respectively, while the NO₂ concentration is 375 ppb, and the NH₃ concentration is 500 ppb. For the oxalic acid particles exposure experiment, the SO₂ concentration is 250 ppb, the NO₂ concentration is 250 ppb, and the NH₃ concentration is 1 ppm (The data of oxalic acid growth are cited from the previous study by Wang et al (2016)).

552
553



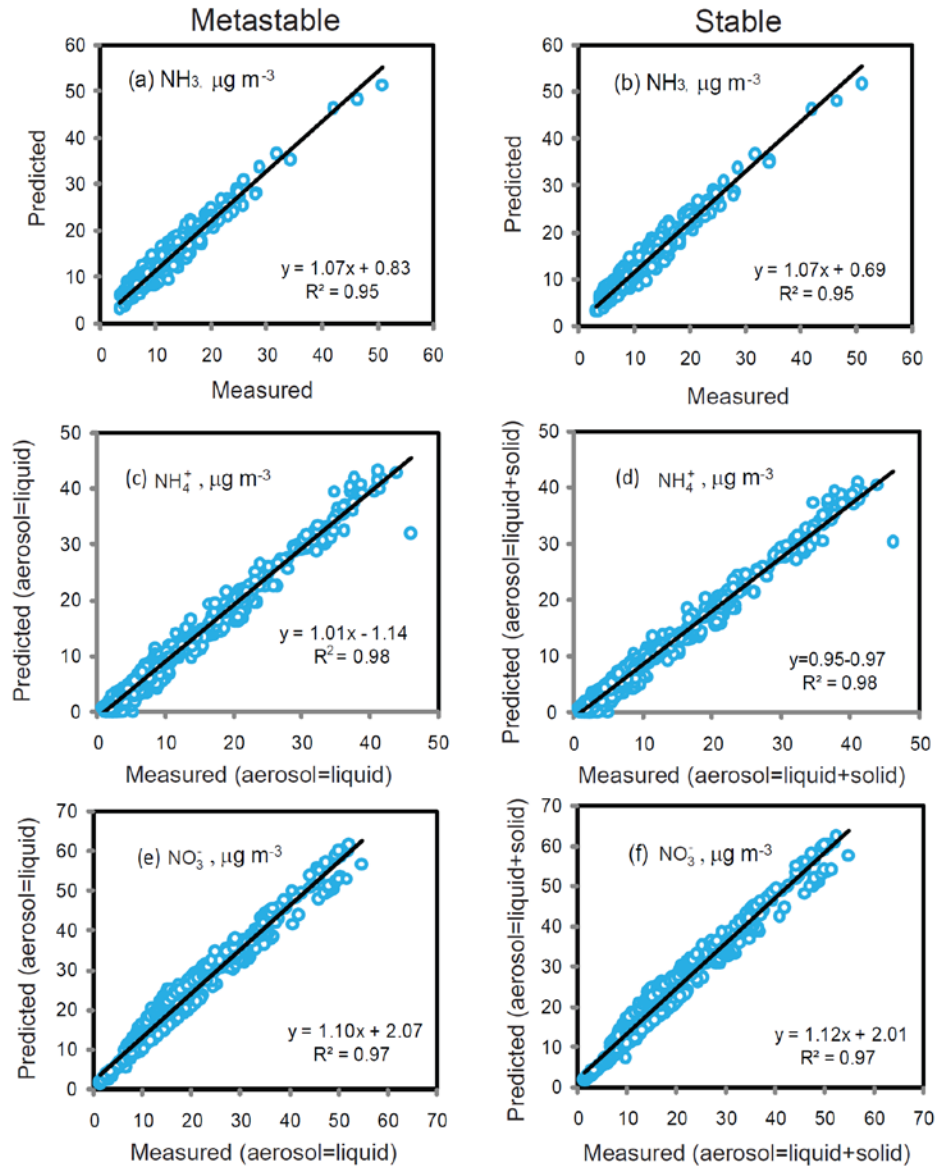
554
555
556 Figure 2. Measured hygroscopic growth factor (HGF) of oxalic acid particles at different RH
557 conditions. D_p is the particle diameter at an elevated RH, and D_0 (100nm) is the initial diameter
558 of oxalic acid particles at RH = 8%.

559
560
561
562
563
564



565
 566
 567
 568
 569
 570
 571
 572

Figure 3. Measurements of water-soluble organic matter (WSOM) of $PM_{2.5}$ collected in Beijing and Hebei Province during the winter of 2016 (left panels: a, c, e and g) and in Xi'an during the winter of 2012 (right panels: b, d, f and h). In (a) and (b), the green, red, blue, yellow, pink, and gray colors represent WSOM, sulfate, nitrate, ammonium, chloride, and the others (i.e., the sum of $Na^+ + Ca^{2+} + Mg^{2+} + K^+$), respectively.



573

574 Figure 4. Comparison of measured NH_3 , NH_4^+ , and NO_3^- concentrations with those predicted by
 575 ISORROPIA-II model using the forward mode under the metastable (left panels) and stable
 576 assumptions (right panels).
 577